RAPID COMMUNICATION

Phonon bottleneck effect due to finite shrinking gap revealed by high-pressure ultrafast dynamics

Yanling Wu(吴艳玲)[1,†], Q. Wu(吴穹)[2,3,†], X. Yin(尹霞)[4], Y. X. Huang(黄逸轩)[2,3], Takeshi Nakagawa[4], Z. Y. Tian(田珍耘)[2], Fei Sun(孙飞)[2,3,5], Q. M. Zhang(张清明)[2,3], Jun Chang(昌峻)[6,‡], Ho-kwang Mao(毛河光)[4], Yang Ding(丁阳)[4,§], and Jimin Zhao(赵继民)[2,3,7,¶]

[1] *State Key Laboratory of Metastable Materials Science and Technology & Hebei Key Laboratory of Microstructural Material Physics, School of Science, Yanshan University, Qinhuangdao* 066004, *China*

[2] *Beijing National Laboratory for Condensed Matter Physics, Institute of Physics, Chinese Academy of Sciences, Beijing* 100190, *China*

[3] *School of Physical Sciences, University of Chinese Academy of Sciences, Beijing* 100049, *China*

[4] *Center for High Pressure Science and Technology Advanced Research, Beijing* 100094, *China*

[5] *Max Planck Institute for Chemical Physics of Solids, Dresden* 01187, *Germany*

[6] *College of Physics and Information Technology, Shaanxi Normal University, Xi'an* 710119, *China*

[7] *Songshan Lake Materials Laboratory, Dongguan, Guangdong* 523808, *China*

(Received 11 November 2025; revised manuscript received 17 December 2025; accepted manuscript online 25 December 2025)

High-pressure ultrafast dynamics has been recently developed, enabling the exploration of non-equilibrium properties of various quantum materials under high pressure. Particularly, by investigating the pressure dependence of time-resolved ultrafast dynamics, we have discovered a pressure-induced phonon bottleneck effect (PBE). To date, all reported PBEs are due to fully closed gaps, which was reflected in the simultaneous characteristic changes in both amplitude and lifetime of the phonon–phonon scattering slow relaxation component. However, as reflected through its connection to Euler disk, incompletely closed gaps can also induce PBEs. In this work, we report the first PBE due to a finite shrinking gap. As is known, it is challenging to directly observe high-pressure-induced variations in electronic band gaps due to the diamond anvil cell. Here, by investigating Sr_2IrO_4 in our previous work, we obtain an empirical formula for the pressure-induced energy gap variation at room temperature. Our quantitative analysis shows that the gap is finite shrinking rather than fully closed.

Keywords: phonon bottleneck effect, ultrafast dynamics, high pressure, ultrafast spectroscopy, finite gap

PACS: 78.47.J–, 62.50.–p, 71.38.–k, 78.47.–p, 87.15.ht

DOI: 10.1088/1674-1056/ae3122 **CSTR:** 32038.14.CPB.ae3122

Time-resolved ultrafast spectroscopy is crucial for gaining the non-equilibrium state and excited-state information of quantum materials.[1–7] It leads to the current research trend ultrafast condensed matter physics.[8,9] Fruitful achievements include the excited-state physical properties,[10,11] non-equilibrium electronic states,[12–14] complex interactions among many degrees of freedom,[4,5,15,16] bosonic collective excitations,[6,16–19] and laser-induced novel states.[6,20–25] The excited-state photo-carrier relaxation exhibits a quasi-diverging lifetime nearby critical order parameters, giving rise to the well-known phonon bottleneck effect (PBE), which is widely observed by ultrafast spectroscopy in superconductors,[12] two-dimensional materials,[6,26] and strongly correlated materials.[17]

The PBE originates from the microscopic dynamic equilibrium between the density of non-equilibrium carriers and high-frequency phonons (HFPs, phonons with an energy large enough to promote the carrier to above the gap), which indicates the onset of a new collective phase and collapse of the energy gap.[12,17,26] This quasi-equilibrium can be broken when the HFPs decay into lower energy elementary excitations or propagate away from the active region.[5,16] Based on Rothwarf–Taylor model,[27,28] Kabanov model,[29] and their extended derivation,[16] critical order parameters such as phase transition temperature and energy gap owing to superconductivity or charge (spin) density wave can be measured directly by ultrafast spectroscopy.[4,5,16,30,31]

Conventionally, the reported PBEs are mostly driven by temperature, and are rarely driven by other external fields. Recently, the combination of high-pressure techniques with time-resolved ultrafast spectroscopy has been realized,[4,7,31–34] which leads to the sophisticated on-site *in situ* investigation of the non-equilibrium quasiparticle (QP) ultrafast dynamics under high pressure. Evidence of strong coupling supercon-

[†]These authors contributed equally to this work.

[‡]Corresponding author. E-mail: junchang@snnu.edu.cn

[§]Corresponding author. E-mail: yang.ding@hpstar.ac.cn

[¶]Corresponding author. E-mail: jmzhao@iphy.ac.cn

© 2026 Chinese Physical Society and IOP Publishing Ltd. All rights, including for text and data mining, AI training, and similar technologies, are reserved.

CPB Online In Press

ductivity and superconducting (SC) gap of $LaH_{10\pm\delta}$ under 165 GPa was obtained by our group.[4] We qualitatively observed the pressure-induced PBE of Sr_2IrO_4 by on-site *in situ* high-pressure ultrafast spectroscopy at room temperature,[7] which corresponds to a gap shrinkage.[10,16]

Intriguingly, according to the transport measurement,[35] there is a gap evolution with finite magnitude. This indicates that the gap is not fully closed, which is distinct from the conventional gap closing of superconductors at their critical temperatures.[5,16] The experimental investigation of the electronic structures of materials at high pressure is challenging due to the space limitation caused by the diamond anvil cell (DAC).[36–38] The pressure-induced PBE measured by ultrafast spectroscopy provides a significant platform for the study of the electronic structure evolution of quantum materials under high pressure.[7]

In this work, we further quantitatively analyze the pressure-induced PBE in Sr_2IrO_4. We explicitly elucidate the physics picture and find that a finite shrinking gap can also induce the PBE. Pressure-induced variations in both amplitude and lifetime of the QPs relaxation are quantitatively analyzed, yielding a concrete finite value of the closing energy gap. Our finding that a finite shrinking gap can lead to the PBE refreshes the conventional understanding of critical phenomena in condensed matters.

Figure 1(a) shows a typical scanning trace of the relative differential reflectivity $\Delta R/R$ of Sr_2IrO_4 at 22.0 GPa. Ultrafast pulses of 800 nm central wavelength, 80 fs pulse duration, and 250 kHz repetition rate were used to excite and probe the ultrafast dynamics.[7] This ultrafast relaxation dynamics exhibits three decay components — the fast, slow, and slowest components. We fit this ultrafast dynamics data with the sum of three exponential decay functions $\Delta R/R = A_{\rm fast}\exp(-t/\tau_{\rm fast}) + A_{\rm slow}\exp(-t/\tau_{\rm slow}) + A_{\rm slowest}\exp(-t/\tau_{\rm slowest})$ with excellent consistency, where $A_{\rm fast}$, $A_{\rm slow}$, and $A_{\rm slowest}$ are the amplitudes of QPs relaxation, and $\tau_{\rm fast}$, $\tau_{\rm slow}$, and $\tau_{\rm slowest}$ are the lifetimes of QPs relaxations, respectively. The red solid curve of Fig. 1(a) is the fitting curve. The three individual exponential components are plotted by blue, orange, and purple solid curves, respectively. The inset of Fig. 1(a) presents the long-range scanning data in the time domain with $\tau_{\rm slowest} = 405$ ps. We attribute these three decay components to the electron–phonon scattering, phonon–phonon scattering, and possible heat diffusion or spin fluctuation, respectively.[7]

The reported transport measurement of Sr_2IrO_4 exhibits a broad "U-shaped" curve in the pressure domain at 50 K.[35,39] In Fig. 1(b), we extracted the resistance values (R) of Sr_2IrO_4 at different pressure (P) at 275 K from Ref. [35]. The value of resistance decreases with increasing pressure from 0 GPa to 20 GPa until reaching a minimum value, after which it remains unchanged from 20 GPa to 30 GPa. At pressures exceeding 30 GPa, the resistance undergoes an increase with increasing pressure. In the inset of Fig. 1(b), we plot the resistance versus pressure (R–P) curve at 275 K in a logarithmic form, which also exhibits a "U-shaped" curve similar to that at low temperature.[35,40] Therein, the lateral size of the Sr_2IrO_4 sample anchored in the DAC is about tens of microns.[35] We estimate the resistivity (ρ) using the equation $R = \rho l/S$, where l denotes the length of the sample, and S represents the area of the sample *ab* plane (the *ab* plane is defined as the plane parallel to the culet of the diamond anvil). As illustrated in Fig. 1(b), the value of resistance for Sr_2IrO_4 at 21.6 GPa and 275 K is 6.0 Ω. We assume that the sample in DAC is a round disk with a radius of 20 μm and the thickness is about 0.2 mm. Consequently, the resistivity is estimated as $\rho \approx RS/l = (6\ \Omega) \times \pi \times (20\ \mu\text{m})^2/(0.2\ \text{mm}) = 3.8 \times 10^{-5}$ (Ω·m). This indicates that the bandgap is not completely closed (i.e., finite gap) at pressure above 20 GPa. There have been research reports that the insulating state of Sr_2IrO_4 even keeps up to 185 GPa.[41]

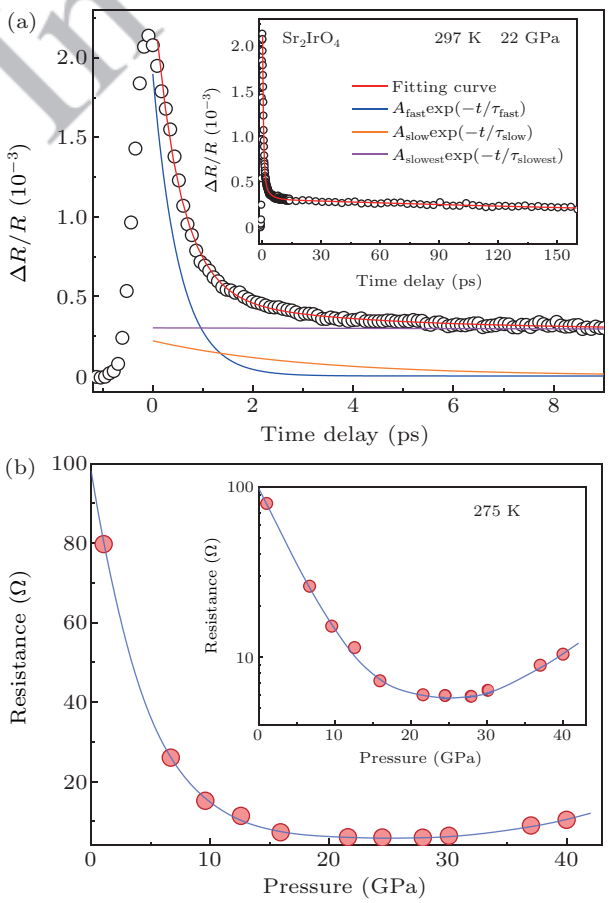

Fig. 1. (a) Typical scanning trace of ultrafast dynamics of Sr_2IrO_4 at 22 GPa and room temperature. Inset: Long-range scanning data of ultrafast dynamics in the time domain. The red solid curve is the fitting curve, and the blue, orange, and purple solid curves are three exponential components of QPs relaxation. (b) Pressure-dependence resistance values of Sr_2IrO_4 at 275 K. Solid curve: guide to the eyes. Inset: the P–R curve in a logarithmic form. The data in panel (b) is reproduced from Ref. [35].

We re-plot the ultrafast relaxation of photocarriers in Sr_2IrO_4 at different pressures in Fig. 2(a) (the data are extracted from our previous work[7]). Among the three decay

CPB Online In-Press

components of QPs relaxation [Fig. 1(a)], the slow component reflects the QPs recombination process across the gap, which is largely dominated by the change of the energy gap.[5,16,30] The quasi-equilibrium state is established between the QPs and phonons, resulting in the simultaneous observation of two prominent changes in amplitude and lifetime determined by the PBE, as shown in Figs. 2(c) and 2(d). As the pressure increases, the amplitude $A_{\rm slow}$ decreases gradually and reaches its minimum value at 20 GPa. Concurrently, the lifetime $\tau_{\rm slow}$ increases gradually and displays divergent-like behaviour at the same pressure. These two simultaneous prominent characteristics are driven by the pressure-induced gap shrinkage near the critical pressure ($P_{\rm c}$), which are analogous to those of the SC phase transitions observed in temperature-dependent ultrafast dynamics experiments.[5,16,28,29] Below $P_{\rm c}$, the excited-state QPs relax to the ground state, releasing the HFPs. Near $P_{\rm c}$, due to the gradually smaller energy gap Δ, more and more HFPs prevent the QPs from relaxing back to the ground state, leading to the greatly enhanced lifetime in the PBE. $A_{\rm slow}$ is proportional to the photo-carrier density that is contributed by the phonon–phonon scattering relaxation channel. Near $P_{\rm c}$, the smaller energy gap sensitively leads to faster single relaxation process, resulting in a decrease in the excited-state carrier density. Thus, $A_{\rm slow}$ decreases with increasing pressure until reaching its minimum value at $P_{\rm c}$.

To quantitatively analyze pressure-induced PBE, we assume the energy gap as a function of pressure as

$$\Delta(P) = \Delta_1 \tanh\left(\vartheta\sqrt{P_{\rm c}/P-1}\right) + \Delta_{\rm c}, \tag{1}$$

where the $\Delta(P)$ is the pressure-induced energy gap, $P_{\rm c}$ is the critical pressure, $\Delta_{\rm c}$ is the gap of the sample at $P_{\rm c}$. The $\Delta_1 + \Delta_{\rm c} = \Delta_0$ is the gap of the sample at the ambient pressure. Δ_1, $\Delta_{\rm c}$ and $P_{\rm c}$ are fitting parameters. ϑ is a parameter reflecting the correlation strength. We write Eq. (1) in a similar way to the previous empirical trial formula.[42] It turns out to be a very effective empirical function in our case, which has been successfully verified in many other investigations too.[4,15,31,42] Analogous to temperature-dependence ultrafast dynamics for superconductors analyzed by the Kabanov model,[5,29] we describe the pressure-dependence amplitude and lifetime of QPs relaxation for the slow decay component as follows:

$$A(P) \propto \frac{1}{[\Delta(P)+k_{\rm B}T/2]\left[1+\gamma\sqrt{2k_{\rm B}T/\pi\Delta(P)}\exp\left(-\Delta(P)/k_{\rm B}T\right)\right]}, \tag{2}$$

$$\tau(P) \propto \frac{\ln\left[\beta/\Delta(P)^2+\exp(-\Delta(P)/k_{\rm B}T)\right]}{\Delta(P)^2}, \tag{3}$$

where γ and β are fitting parameters, $T = 297$ K is the sample temperature in our experiment. We fit the experimental data in Figs. 2(c) and 2(d) (red curves) using Eqs. (2) and (3), yielding that $\Delta_1 = 79$ meV, $\Delta_{\rm c} = 88$ meV, $P_{\rm c} = 20$ GPa, and the correlation parameter $\vartheta = 1.78$. Thus, the energy gap at ambient pressure is obtained to be $\Delta_0 = 167 \pm 4$ meV, which is consistent with the reported values in Refs. [39,43,44]. According to our data analysis, the energy gap is reduced to 88 ± 2 meV at 20 GPa. To clearly test and illustrate the reliability of the data analysis results, we performed trial fit with the critical pressure fixed at 19 GPa (blue curves) and 21 GPa (cyan curves), respectively. The red curves (20 GPa) are the most consistent with the experimental data [Figs. 2(c) and 2(d)]. The trial results are not the best fittings. Therefore, the critical pressure is estimated to be $P_{\rm c} = 20 \pm 1$ GPa.

From the fitting results, we obtained the energy gap of Sr_2IrO_4 as a function of pressure as $\Delta(P) = 79\tanh\left(1.78\sqrt{20/P-1}\right) + 88$ meV, which is plotted in Fig. 2(b) (red curve). The insulating gap can be estimated by transport measurement using the relation $\rho \propto \exp\left(E_{\rm g}/2k_{\rm B}T\right)$,[35] where $E_{\rm g}$ is the energy gap, $k_{\rm B}$ is the Boltzmann constant. Thus, we derived the gap value by fitting the temperature-dependent resistance value from 250 K to 300 K at different pressures, adapted from Ref. [35], which is plotted in Fig. 2(b) (blue spheres). The gap equation that we adopted yields pressure-dependent gap values (red curve) that are consistent with all the derived gap values from resistance measurement (blue spheres) for the whole pressure range. Thus, the gap formula at room temperature is an excellent fitting equation for our case. The applicability of this formula to different temperatures needs to be investigated in the future.

Usually, the electronic energy bands will approach each other under high pressure.[36,40] High enough pressure can induce an insulator-to-metal transition, due to the overlap of electronic bands.[36,40] That the energy gap of Sr_2IrO_4 shrinks with increasing pressure has been evidenced by the resistance measurement[35] and the ultrafast spectroscopy measurement.[7] Notably, the gap does not continuously decrease with increasing pressure. It was reported that there was no abrupt change of structure in the regime of 0–25 GPa for Sr_2IrO_4.[35,39] Above 30 GPa, the resistance value is reported to increase[35] rapidly, accompanied by a pressure-induced structural distortion (from the native tetragonal $I4_1/acd$ phase to an orthorhombic $Pbca$ phase), which leads to a persistent insulating state up to megabar pressures.[41]

CPB Online In-Press

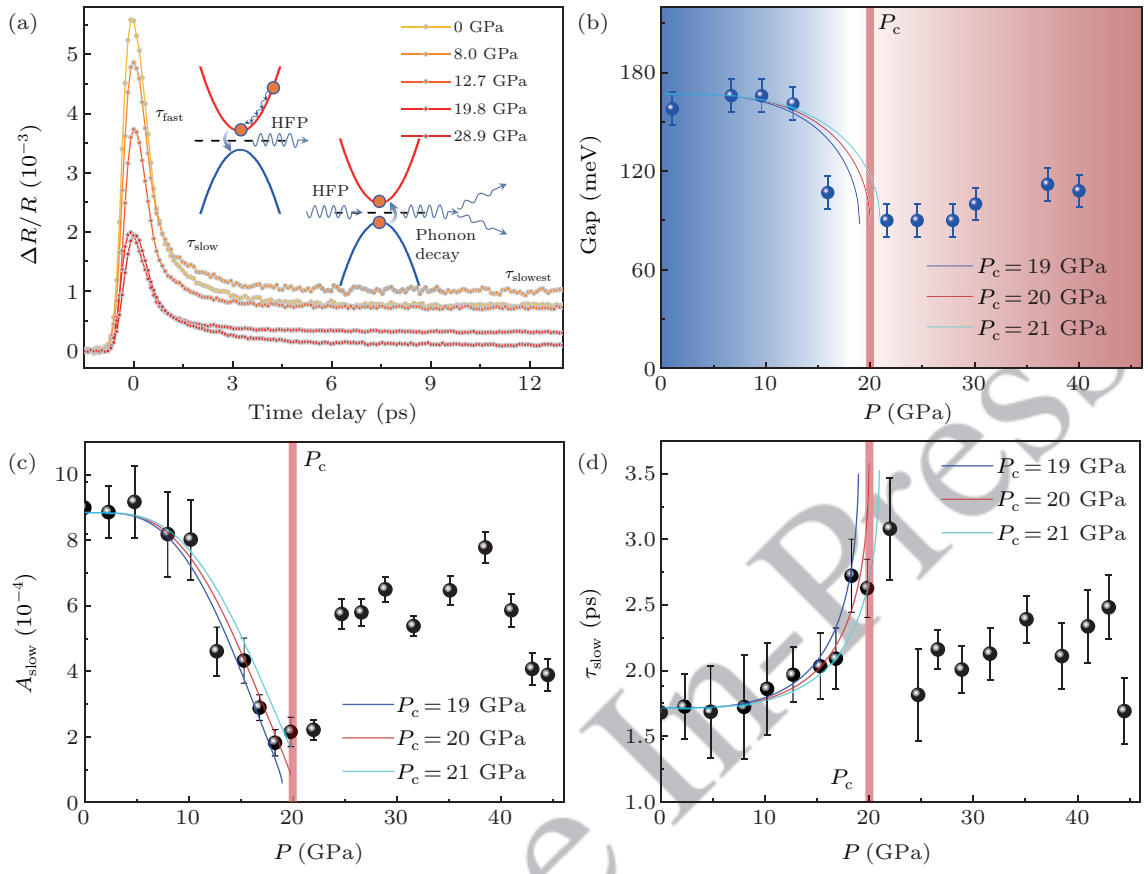

Fig. 2. (a) Pressure dependence of the typical ultrafast dynamics of Sr_2IrO_4. Inset: Schematic diagram of the QPs relaxation physical processes, corresponding to the slow decay component. (b) Pressure dependence of energy gap. Data (blue spheres) are reproduced from Ref. [35] by transport measurement. Solid curves: energy gap formula corresponding to the fitting curves in panels (c) and (d). (c) and (d) Pressure dependences of the amplitude A_{slow} and lifetime τ_{slow} of ultrafast QPs relaxation for slow component. Solid curves: fitting results using Eqs. (2) and (3). Data in panels (a), (c), and (d) are reproduced from Ref. [7].

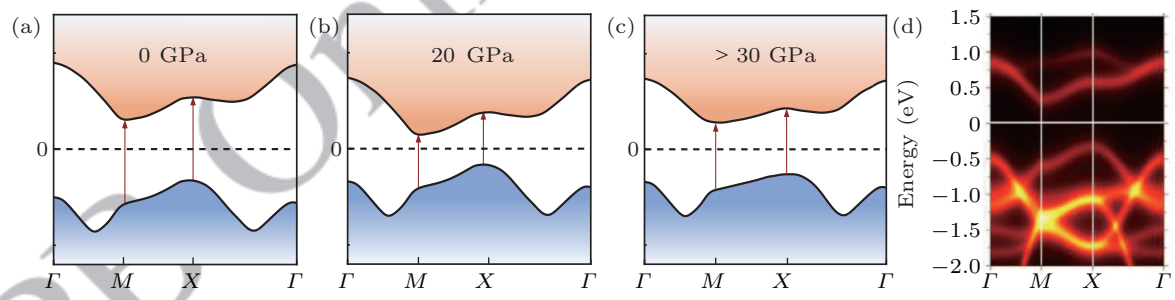

Fig. 3. Schematic diagram of the proposed electronic band structure evolution of Sr_2IrO_4. (a) At ambient pressure, referring to Ref. [45], (b) at the pressure of 20 GPa, and (c) above 30 GPa. (d) Calculated momentum-resolved spectral function of Sr_2IrO_4, reproduced from Ref. [45].

We propose a physical picture of the band evolution of Sr_2IrO_4 along with increasing pressure. In Fig. 3(a), we present the schematic of electronic band structure of Sr_2IrO_4 at ambient pressure, as investigated in Ref. [45], where the energy gap is signified at around X and along the X–M line in the momentum space. This is based on the reported results in Ref. [45], from which we adapt and replot a figure as Fig. 3(d). As the pressure increases, the top of the lower Hubbard band (LHB) and the bottom of the upper Hubbard band (UHB) of the $J_{eff} = 1/2$ Mott state[40] gradually approach each other [Fig. 3(b)], which causes a shrinkage in the band gap when approaching 20 GPa. Note that, however, the resistance value [Fig. 1(b)] and energy gap [Fig. 2(b)] of Sr_2IrO_4 are nearly unchanged between 20 GPa and 30 GPa, and begin to increase above 30 GPa. Above 30 GPa, there might be potential band distortion near the Fermi surface, associated with the enhancement of the gap value [Fig. 3(c)]. When the effect of the distortion is larger than the band proximity caused by pressure, the energy gap may increase with pressure. The bottom of the UHB and the top of the LHB shift oppositely due to the band deformation, which enhances the gap [Fig. 3(c)] above 30 GPa.

Finally, in our previous investigation, we found that microscopic PBE and macroscopic Euler disk are indeed the two sides of one coin, both being intrinsic for excited-state physics. The decreasing and quasi-divergent behaviors of PBE in am-

CPB Online In Press

plitude (i.e., carrier density) and lifetime are similar to those of a classical Euler disk in energy and frequency.[10] The ordering parameter for PBE is temperature or pressure, while that for the Euler disk is time. Here, it is pedagogical to contemplate from the Euler disk whether a finitely closed gap can lead to PBE. Taking the Euler disk as an analogy, a finite gap corresponds to the state where the coin is right before falling down completely to the ground. In this case, most of the features of the Euler disk still remain: the frequency tends to dramatically enhance and the energy is decreasing. Hence, from the insightful analogy from the Euler disk, PBE due to finite-shrinking gap is fully possible.

In summary, we quantitatively investigate the pressure-induced PBE in Sr_2IrO_4, which is due to a shrinking but finite gap. All previously reported PBEs induced by temperature are due to fully closed gaps. We proposed an empirical formula to describe the variation of energy band gap driven by pressure at room temperature. We obtained the energy gap of 167 ± 4 meV at ambient pressure, which was reduced to 88 ± 2 meV at 20 GPa. Our quantitative analysis demonstrates that a shrinking but finite gap is also capable of inducing the PBE, which enriches the conventional understanding of critical phenomena in condensed matters.

Acknowledgments

Project supported by the National Natural Science Foundation of China (Grant Nos. 12204400 and 12534006), Beijing National Laboratory for Condensed Matter Physics (Grant No. 2024BNLCMPKF020), Innovation Capability Improvement Project of Hebei Province (Grant No. 22567605H), the National Key Research and Development Program of China (Grant Nos. 2024YFA1408700 and 2021YFA1400201), and CAS Project for Young Scientists in Basic Research (Grant No. YSBR-059).

References

[1] Giannetti C, Capone M, Fausti D, Fabrizio M, Parmigiani F and Mihailovic D 2016 *Adv. Phys.* **65** 58
[2] Kirilyuk A, Kimel A V and Rasing T 2010 *Rev. Mod. Phys.* **82** 2731
[3] Torre A D, Kennes D M, Claassen M, Gerber S, McIver J W and Sentef M A 2021 *Rev. Mod. Phys.* **93** 041002
[4] Wu Y L, Yu X H, Hasaien J Z L, Hong F, Shan P F, Tian Z Y, Zhai Y N, Hu J P, Cheng J G and Zhao J M 2024 *Nat. Commun.* **15** 9683
[5] Tian Y C, Zhang W H, Li F S, Wu Y L, Wu Q, Sun F, Zhou G Y, Wang L L, Ma X C, Xue Q K and Zhao J M 2016 *Phys. Rev. Lett.* **116** 107001
[6] Hasaien J, Wu Y L, Shi M Z, Zhai Y N, Wu Q, Liu Z, Zhou Y, Chen X H and Zhao J M 2025 *Proc. Natl. Acad. Sci. USA* **122** e2406464122
[7] Wu Y L, Yin X, Hasaien J, Ding Y and Zhao J M 2020 *Chin. Phys. Lett.* **37** 047801
[8] Hao W J, Zhai Y N, Dai Z J, Zhang H and Zhao J M 2024 *Chin. Sci. Bull.* **69** 3177
[9] Zhao J M 2026 *Chin. Phys. Lett.* **43** 030710
[10] Lin X N, Fu S H, Zhai Y N, Wang W H, Li H C, Zhang R Z, Meng S and Zhao J M 2024 *Innovation* **5** 100614
[11] Jiang L T, Jiang C Y, Tian Y C, Zhao H, Zhang J, Tian Z Y, Fu S H, Liang E J, Wang X C, Jin C Q and Zhao J M 2024 *Chin. Phys. Lett.* **41** 047802
[12] Wu Q, Tian Y C, Wu Y L and Zhao J M 2017 *Chin. Sci. Bull.* **62** 3995
[13] Wang R, Ding J W, Sun F, Zhao J M and Qiu X H 2024 *Chin. Phys. Lett.* **41** 057801
[14] Zhang E R, Yao J S, Geng Z M, Hou Y Y, Dai J Y and Lu H 2025 *Chin. Phys. Lett.* **42** 028501
[15] Cheng Y, Zhou F R, Teng J, Li P Y, Jiang L T, Gong P M, Li Y Q, Wu X J, Kärtner F X and Zhao J M 2025 *Nat. Commun.* **16** 5656
[16] Wu Q, Zhou H X, Wu Y L, Hu L L, Ni S L, Tian Y C, Sun F, Zhou F, Dong X L, Zhao Z X and Zhao J M 2020 *Chin. Phys. Lett.* **37** 097802
[17] Zhai Y N, Gong P M, Hasaien J, Zhou F R and Zhao J M 2024 *Prog. Surf. Sci.* **99** 100761
[18] Dong T, Zhang S J and Wang N L 2023 *Adv. Mater.* **35** 2110068
[19] Hao W J, Gu M H, Tian Z Y, Fu S H, Meng M, Zhang H, Guo J D and Zhao J M 2024 *Adv. Sci.* **11** 2305900
[20] Zeng Z, Först M, Fechner M, Amuah E B, Putzke C, Moll P J W, Prabhakaran D, Radaelli P G and Cavalleri A 2025 *Science* **387** 431
[21] Stojchevska L, Vaskivskyi I, Mertelj T, Kusar P, Svetin D, Brazovskii S and Mihailovic D 2014 *Science* **344** 177
[22] Wu Y, Wu Q, Sun F, Cheng C, Meng S and Zhao J 2015 *Proc. Natl. Acad. Sci. USA* **112** 11800
[23] Huang Y X, Zhao H, Li Z L, Hu L L, Wu Y L, Sun F, Meng S and Zhao J M 2023 *Adv. Mater.* **35** 2208362
[24] Li J, Niu W S, Xu X D, Wang M, Xu Z W, Cao J W, Li J M, Zhao J M and Wu Y L 2025 *Opt. Express* **33** 1044
[25] Choi D, Yue C, Azoury D, Porter Z, Chen J, Petocchi F, Baldini E, Lv B, Mogi M, Su Y, Wilson S D, Eckstein M, Werner P and Gedik N 2024 *Proc. Natl. Acad. Sci. USA* **121** e2323013121
[26] Jin C, Ma E Y, Karni O, Regan E C, Wang F and Heinz T F 2018 *Nat. Nanotechnol.* **13** 994
[27] Rothwarf A and Taylor B N 1967 *Phys. Rev. Lett.* **19** 27
[28] Kabanov V V, Demsar J and Mihailovic D 2005 *Phys. Rev. Lett.* **95** 147002
[29] Kabanov V V, Demsar J, Podobnik B and Mihailovic D 1999 *Phys. Rev. B* **59** 1497
[30] Chia E E M, Talbayev D, Zhu J X, Yuan H Q, Park T, Thompson J D, Panagopoulos C, Chen G F, Luo J L, Wang N L and Taylor A J 2010 *Phys. Rev. Lett.* **104** 027003
[31] Meng Y H, Yang Y, Sun H L, Zhang S S, Luo J L, Chen L C, Ma X L, Wang M, Hong F, Wang X B and Yu X H 2024 *Nat. Commun.* **15** 10408
[32] Tu H Y, Pan L Y, Qi H J, Zhang S H, Li F F, Sun C L, Wang X and Cui T 2023 *J. Phys. Condens. Matter* **35** 253002
[33] Wu Y L, Yin X, Hasaien J Z L, Tian Z Y, Ding Y and Zhao J M 2021 *Rev. Sci. Instrum.* **92** 113002
[34] Hasaien J Z L, Shan P F, Zhou F R and Zhao J M 2025 *Rev. Sci. Instrum.* **96** 013004
[35] Haskel D, Fabbris G, Zhernenkov M, Kong P P, Jin C Q, Cao G and Veenendaal M V 2012 *Phys. Rev. Lett.* **109** 027204
[36] Mao H K, Chen X J, Ding Y, Li B and Wang L 2018 *Rev. Mod. Phys.* **90** 015007
[37] Ding Y, Yang L, Chen C C, Kim H S, Han M J, Luo W, Feng Z, Upton M, Casa D, Kim J, Gog T, Zeng Z and Cao G 2016 *Phys. Rev. Lett.* **116** 216402
[38] Du F, Drozdov A P, Minkov V S, Balakirev F F, Kong P, Smith G A, Yan J F, Shen B, Gegenwart P and Eremets M I 2025 *Nature* **641** 619
[39] Zocco D A, Hamlin J J, White B D, Kim B J, Jeffries J R, Weir S T, Vohra Y K, Allen J W and Maple M B 2014 *J. Phys. Condens. Matter* **26** 255603
[40] Cao G and Schlottmann P 2018 *Rep. Prog. Phys.* **81** 042502
[41] Chen C H, Zhou Y H, Chen X L, Han T, An C, Zhou Y, Yuan Y F, Zhang B, Wang S Y, Zhang R R, Zhang L L, Zhang C J, Yang Z R, DeLong L E and Cao G 2020 *Phys. Rev. B* **101** 144102
[42] Wang Z S 2012 *Phys. Rev. B* **86** 060508
[43] Kim B J, Jin H, Moon S J, Kim J Y, Park B G, Leem C S, Yu J, Noh T W, Kim C, Oh S J, Park J H, Durairaj V, Cao G and Rotenberg E 2008 *Phys. Rev. Lett.* **101** 076402
[44] Ge M, Qi T F, Korneta O B, DeLong D E, Schlottmann P, Crummett W P and Cao G 2011 *Phys. Rev. B* **84** 100402
[45] Martins C, Lenz B, Perfetti L, Brouet V, Bertran F and Biermann S 2018 *Phys. Rev. Mater.* **2** 032001

CPB Online First